Journal of Thermal Analysis, Vol. 5 (1973) 533–550

A NEW METHOD OF DTA: THEORY AND PRACTICE

N. H. Sze and G. T. Meaden*

Research Centre of National Iron and Steel Mills Ltd.
*Republic of Singapore, 22; *Artetech International, Bath, BA2 5DW, England*

(Received April 3, 1972; in revised form September 25, 1972)

A novel differential thermoanalytical technique is described and discussed with regard to function, operation, performance, theory and application. Information is provided about the nature of the internal processes taking place at the time of absorption or release of energy. Notable features of the technique include high sensitivity and independence of a reference sample.

Over the years, since the pioneering work of Roberts-Austen [1, 2] Le Chatelier [3, 4], and others [5] at the turn of the century, DTA has been put to extensive and varied use in science and industry. From the technical standpoint much attention has been directed at increasing the sensitivity and reproducibility of the method, and this has led to the development of elaborate and sophisticated automatic recording techniques. The fundamental principle of comparison with a reference material has been maintained throughout this period. Nevertheless there are certain difficulties which are unavoidable with this technique. On the one hand there are problems associated with the selection of a suitable reference material and on the other hand with the requirement that both the substance and the reference should be exposed to identical environmental conditions. This requirement necessitates that, ideally, there should be insignificant temperature gradients across the specimens and between them. These basic difficulties are met by the new approach to DTA presented here.

In this method, because the test sample itself is used as its own reference, no separate reference material is necessary. The requirement for eliminating temperature gradients disappears because by contrast with conventional DTA, a deliberately-imposed temperature gradient along the sample is obligatory. Moreover, by means of this technique, a new type of effect taking place at first-order phase transitions is revealed. A distinctive thermoanalytical curve characteristic of the method is produced, and its analysis gives physical information about internal microscopic processes which are new to thermal analysis. The method should be of particular value when used in conjunction with conventional DTA as a means of obtaining more complete differential thermal information about the physical and chemical processes occurring within materials. Brief descriptions of the new method have been announced in publications elsewhere [6–8]. The present paper provides a more complete mathematical and physical account and includes much additional material (see also reference [9]).

Technique

As with conventional DTA, the sample to be investigated is mounted either in a furnace or in a cryostat containing a heater, whose power adjustment allows the sample and its environment to be raised or lowered in temperature at a controlled rate.

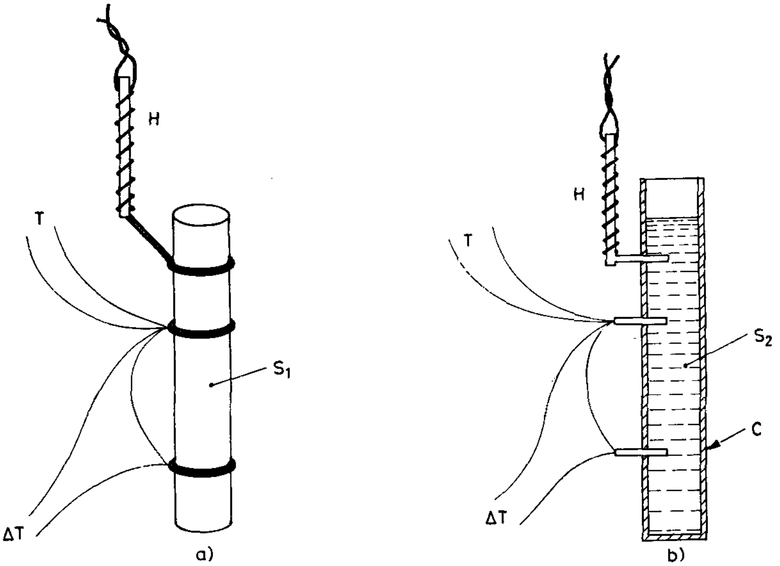

Fig. 1. Disposition of the heater and thermocouples for (a) solid samples (S_1), (b) powdered or liquid samples (S_2). H = heater, C = container of poor thermal conductivity, T = upper thermocouples, ΔT = differential thermocouples

Samples of any shape may in principle be studied, but there is a practical convenience in working with cylindrical samples. A typical sample might be a solid rod such as S_1 (in Fig. 1(a)), or a powder or liquid such as S_2 (in Fig. 1(b)) held in a tube C made from a material of poor thermal conductivity, such as pyrophyllite or polyethylene. The sample is mounted vertically with a small wire-wound resistance heater H firmly secured to its upper end. The means of attachment varied according to the sample and the temperature range of investigation, but for the various solid substances that we have studied (metals and nonmetals) spot-welded, soldered, or epoxy-resined joints were satisfactory. For liquid or powder samples the heater support passed through the wall of the container and into the sample itself.

The sample heater is used to establish a temperature gradient along the sample length which, in the absence of an exothermic or endothermic reaction, provides the thermoanalytical curve with a base-line of operation. This base-line temperature-gradient is monitored by a differential thermometric pair, such as thermocouples, attached to the sides of the sample. We have employed various temperature gradients in the tests ranging from about 0.5 deg to over 10 deg K. On occasions, we have created the desired temperature gradient by locating the sample in an inhomogeneous temperature region of the apparatus, and dispensed with the sample heater. The microvolt signal from the differential thermocouple pair, when determined manually, was measured using a Leeds and Northrup K5 microvolt potentiometer with a DC electronic null detector. In such experiments copper-constantan thermocouples were used.

In other experiments an automatic arrangement was used in which the microvolt signal was recorded on a Texas Instruments dual-channel strip-chart recorder after suitable amplification using the sensitive, low-noise microvolt amplifier which forms part of the Fisher Company's Series 300 modular quantitative differential thermal analyser (QDTA). In this part of our work we used the linear programmer and furnace from the same system together with platinel thermocouples (as used in the Fisher 300 QDTA).

The effect

Figs 2 and 3 illustrate the effect observed at melting and freezing transitions of metallic elements. Fig. 2 is an example of data obtained manually and relates to mercury whose melting point is close to 234°K.

The mercury which was 99.9999% pure was purchased from Koch-Light Laboratories Ltd., Colnbrook, England. The 5.6 cm long sample was contained in a thin-walled polyethylene tube of 0.8 cm internal diameter. Two thermocouples made thermal contact, 3.6 cm apart, with the sample via short platinum wires such that the distance from each thermocouple junction to the mercury was about 3 mm (Fig. 1(b)). An inert gas atmosphere of about 10^{-4} torr helium was maintained in the cryostat, and the rate of heating through the transition was about 0.1°/min. Certain other physical details regarding the sample are supplied in the next section with a theoretical analysis of Fig. 2.

Within the region of temperature where no evolution or absorption of energy takes place, the thermoanalytical curve is uniform (as on the extreme left-hand and right-hand sides of each part of the figure). But when a release or intake of energy occurs within the specimen, the curve is modified in a characteristic manner as indicated by the twin-peak part of each graph. It will be shown in the next section that (i) the minimum in Fig. 2(a) occurs when the advancing liquid/solid phase boundary reaches the location of the first thermocouple probe (i.e. the thermocouple which is nearest the heater); (ii) the maximum point of the curve corresponds to the arrival of the phase boundary at the second thermocouple; and

(iii) the melting temperature for the sample, under the conditions of the experiment, is given approximately by the mean of the graph temperatures for $\Delta T_{\min}$ and $\Delta T_{\max}$. The twin-peak effect is a direct consequence of the additional heat current caused by the motion of the instantaneous internal heat sources when superposed on the main current due to the sample heater. At the same time, it will be understood why on this type of thermoanalytical curve the pair of opposed extrema have their senses inverted for cooling runs compared with heating runs.

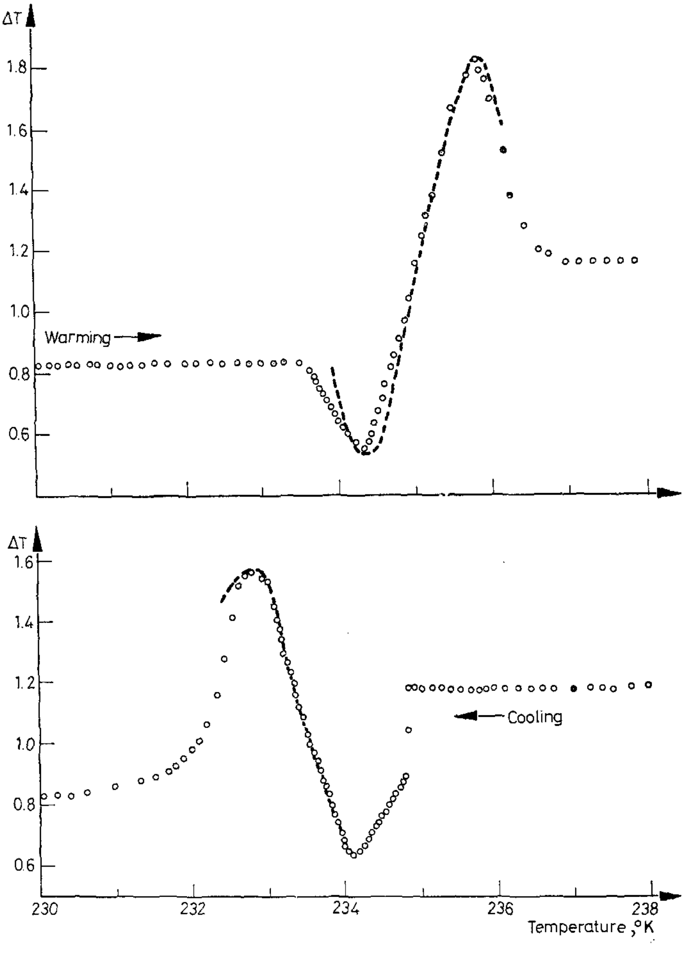

Fig. 2. Mercury $\Delta T - T$ curves obtained by the manual method. Note the mutual reversal of the twin-peaks for cooling compared to warming. The dotted lines are theoretical curves discussed in Section 4

Fig. 3 is supplied as an example of a curve obtained by the automatic recording technique. The data were obtained for the melting and subsequent refreezing of high-purity (99.9999%) indium. The normal melting point is 156°C. The sample was contained in a thin-walled pyrophyllite tube, of internal diameter 0.7 cm, with air at normal pressure as the surrounding atmosphere. The separation of the probes of the differential thermocouple pair was about 2.0 cm. The rate of heating was programmed for 10°/min and the rate of cooling for 10°/min, using a chart speed of 2.5 cm/min. The basic features of the thermal curves in the phase transition region are closely similar to the preceding ones for mercury, with one notable exception. The mutual inversion of the extrema of the thermoanalytical curve, noted in Fig. 2 for cooling compared with heating, does not appear in Fig. 3. This is because of the different abscissae used for the two figures. The abscissae of Fig. 3, being taken from a chart record, represent *increasing time*, with no regard as to whether the temperature is rising or falling in contrast to the abscissae of Fig. 2.

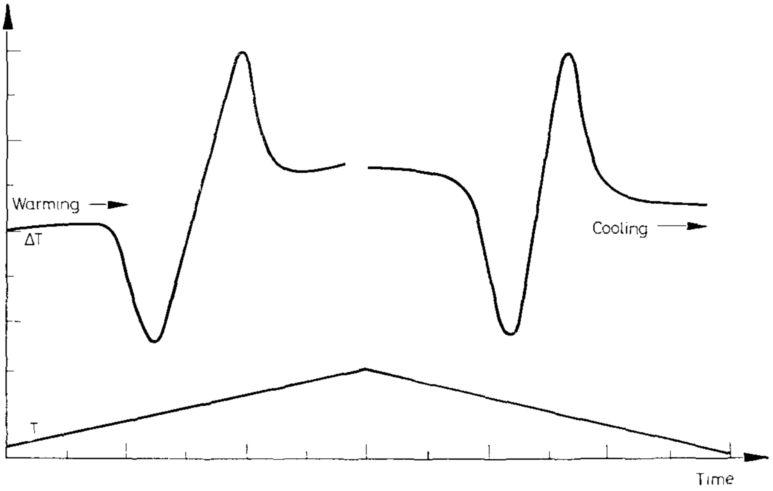

Fig. 3. Indium ΔT-time curves produced on a chart recorder. The form of the peaks is the same for endothermic and exothermic reactions

These two figures illustrate the main characteristics of the twin-peaked effect which appears in the ΔT signal whenever a sample, across which there exists a temperature gradient, undergoes a transformation involving the release or absorption of heat. Essentially similar curves were obtained in all our work which concerned solid and powdered metallic, inorganic and organic substances at their melting and freezing points and at crystal structure transformation temperatures. The only restriction to this statement is that for liquid $\rightleftarrows$ solid changes if the solid density exceeds the liquid density it is preferable to ensure that the direction of heat flow is the same as the earth's gravitational field. Otherwise, complications can arise, if the lower end of the sample melts first, due to convection and surface tension effects.

Phenomenological theory

The twin-peak effect originates from the generation of a heat source or sink over the surface region separating the hotter and cooler phases within the test substance and from the subsequent propagation of this heat through the remainder of the sample. In the case of first-order phase transitions (crystallographic rearrangements, changes of state, etc.), the heat evolved or absorbed is the latent heat. The development of the twin-peaks is described using a phenomenological model, developed from standard heat-conduction theory, for the propagation of an instantaneous plane source of heat evolved or absorbed per unit area of the specimen cross-section.

The temperature distribution, T, in a solid or stationary liquid through which heat is flowing is described in standard references such as Carslaw and Jaeger [10] by

$$\rho C_p \frac{\partial T}{\partial t} = K \nabla^2 T$$

where ρ is the density, C_p is the specific heat, K is the thermal conductivity, and t is time. For one-dimensional heat flow with constant thermal properties in both the solid (S) and liquid (L) regions, the applicable differential equations are $\partial T_S/\partial t = \alpha_S(\partial^2 T_S/\partial x^2)$ and $\partial T_L/\partial t = \alpha_L(\partial^2 T_L/\partial x^2)$, if internal natural convection can be neglected. α_S and α_L are the thermal diffusivities for the solid and liquid regions respectively. When a substance of a single component or eutectic composition changes its state, the heat balance across the surface of separation at $x = s(t)$ is $K_S(\partial T_S/\partial x) = K_L(\partial T_L/\partial x) + \rho Q(\mathrm{d}S/\mathrm{d}t)$, where Q denotes the latent heat. The essential feature of such problems is the existence of a moving surface of separation between the two phases. The way in which this surface moves has to be determined. Heat is liberated or absorbed on it and the thermal properties of the two phases on opposite sides may be different as well.

The application of solutions to the unsteady heat conduction problem with change of phase has great practical importance. For example, the problem of ice formation is significant both in geophysics and in ice manufacture; much attention has been given to the solidification of castings; in aerospace studies the problem of ablation is encountered when a body moves with hypersonic velocity through the earth's atmosphere. Yet there exist relatively few solutions which may be extended to practical cases. The characteristic feature of the problem is the coupling of the temperature field with the rate of propagation of the interface between the solid and liquid phases, which makes the problem non-linear. Only a few exact analytical solutions have been found for special cases. For example, Neumann's solution (see Carslaw and Jaeger [10]) relates to the solidification of the semiinfinite region of a liquid, initially above or at the fusion temperature, when the surface wall temperature is suddenly decreased to and maintained at a temperature below the point of fusion. Analytical solutions are limited by mathematical complexity, while most numerical solutions have not been developed in a convenient, general yet accurate form [11]. However, electrical analogues like the resistance-network analogue, have proved useful for studying heat conduction problems with change of phase [12]. With our experimental arrangement, the measurable parameter connected with the "latent heat" is simply the temperature difference (ΔT). The result of our effect can be calculated theoretically if we treat our case as the analogue of the "heat pulse method for the measurement of thermal diffusivity". This analogy is physically and mathematically reasonable under certain assumptions.

The 'pulse method' for measuring the thermal diffusivity of metals was first suggested by Woisard [13] and further developed by Oualid [14], and Foley and Sawyer [15]. The basic principle can be understood by considering an infinitely long, thin rod lying along the x-axis. If this rod experiences no thermal gains or losses and all heat flow is parallel to the x-direction, the diffusion equation reduces to $\partial T/\partial t = \alpha(\partial^2 T/\partial x^2)$ where T is the temperature of the rod at the point x and time t. Because the rod is at a uniform temperature, the differential-temperature base-line can be considered zero. At $t = 0$, a momentary *heat pulse* is generated in the centre plane of the rod, $x = 0$, such that the initial temperature distribution along the rod is $T(x, t = 0) = T_0\delta(x)$ where $\delta(x)$ is the delta function, with the properties that

$$\int_{-\infty}^{\infty} \delta(x)\mathrm{d}x = 1, \quad \delta(x)\begin{cases} 0 & \text{as } x \neq 0 \\ \infty & \text{as } x \to 0 \end{cases}$$

Then the boundary condition is that $\lim\limits_{x \to \pm\infty} T(x, t) = 0$. This means that the temperature of the rod at points far from $x = 0$ approaches zero. The solution is given by Carslaw and Jaeger [10], Fourier [16] and Luikov [17] as

$$T(x, t) = T_0(4\pi\alpha t)^{-1/2} \exp(-x^2/4\alpha t) \tag{1}$$

In Woisard's [13] experiments, a heat pulse was generated at one end of the thin sample rod by discharging a bank of capacitors across the circuit containing the rod and a small silicon carbide heater-disc. Woisard found the initial temperature distribution to be essentially a square pulse in the region of the heater element instead of the delta function for the ideal case, i.e. the boundary condition of Eq. (1) should be written

$$T(x, t = 0) = 0 \quad \text{for } x < -\frac{d}{2} \text{ and } x > \frac{d}{2}$$

$$= T_0 \quad \text{for } -\frac{d}{2} < x < \frac{d}{2}$$

where the thickness of the heater disc is d. This leads to a solution of Eq. (1) which may be written in the form

$$\lim_{d(4\pi\alpha t)^{-1/2}\to 0} T(x,t) = T_0 d(4\pi\alpha t)^{-1/2}\exp(-x^2/4\alpha t) \tag{2}$$

In our problem, a constant heat current is applied along the sample rod. Within the single-phase temperature region (either solid or liquid), a constant temperature gradient is obtained, and over a short temperature interval, the thermal properties of the sample are almost unchanged. Therefore, on the ΔT vs T_{mean} plot (Fig. 4), two almost horizontal straight lines result in the solid and liquid states. The slight difference in magnitude is caused by the different thermal properties of the two phases. As T_{mean} decreases or increases uniformly through the interfacial region, the distinctive curve with its twin peaks (as illustrated in Fig. 4 by the dotted line) is observed experimentally. Physically, the extrema correspond to the passage of the interfacial phase boundary (acting as the internal sources or sinks of latent heat) past each thermometer in turn. The mutual inversion of their extrema, when comparing the cooling result with the warming one, is due to the reversible property of the "latent heat" (which is exothermic during cooling and endothermic during warming). In either case they are the direct consequence of the extra heat current caused by the motion of these heat sources or sinks superposed on the main heat current due to the sample heater. The following development of the

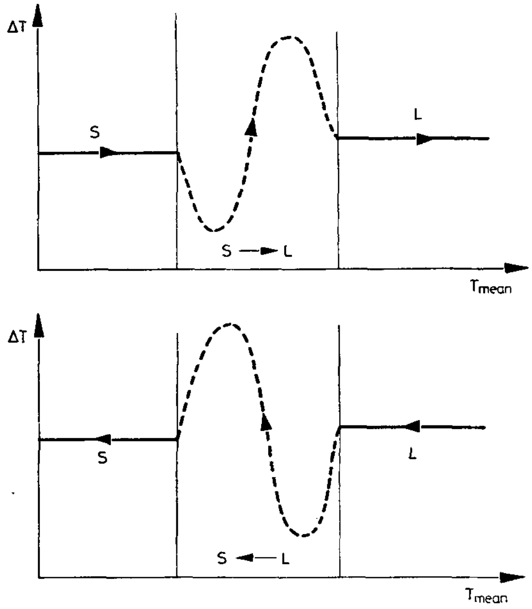

Fig. 4. Idealised $\Delta T - T$ curves for endothermic and exothermic reactions

calculation is based on these qualitative facts and also considers only the change of the dotted-line portion in Fig. 4 with respect to the almost constant horizontal ΔT-base line.

It is well-known that during the melting or freezing of metals in the presence of a temperature gradient, the interfacial phase boundary often moves intermittently even with constant continuous driving force acting on the phase boundary [18–25]. During the freezing process, for example, the interface, instead of moving steadily changes its rate almost periodically. By recording the motion of the crystallization front of bismuth and lead automatically on a photographic plate, it has been found that this intermittent motion is practically simple harmonic with period $2\tau'$ (a few seconds) and amplitude $d(\sim 10^{-2}\,\text{cm})$ [23, 26–28].

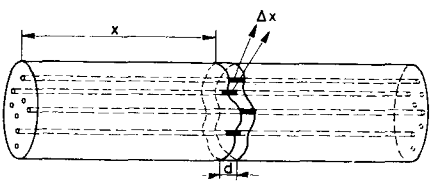

Fig. 5. Division of a long, thin cylindrical specimen into n elementary thin rods.

We consider a long thin cylindrical sample, having, say, a length of a few cm and a diameter of a few mm. It is insulated from the surroundings, and any change of the cross-sectional area with distance along the x-axis is negligibly small. With these assumptions, the problem can be treated as almost one-dimensional. We further assume that the densities of the liquid and solid phases are kept constant and that convection in the liquid phase is negligible. In order to approach the ideal one-dimensional case still more closely, the thin cylinder is subdivided into n elementary thin rods (Fig. 5). Suppose that during the period of crystallization $\tau'(t_1 \rightarrow t_2)$, $n_1(<n)$ elementary rods, with their individual interfaces at positions x freeze and advance a distance Δx.* Latent heat is evolved from these n_1 elementary heat sources; together with the non-frozen $(n - n_1)$ elements, this constitutes the non-planar interface observed in experiments under the microscope. Here, we ignore the detailed structure of the interface and consider that the total heating effect (caused by the latent heat evolution) will be the same as if the interface advances, on average, an effective distance $d(d \sim \Delta x)$. In other words, during the time interval $t_2 - t_1$ a certain amount of heat is generated by a *single* heat source within a slice of thickness d. As the interface moves forward in a harmonic manner (with the rate changing periodically, as mentioned above, even when subjected

---

* In the case of magnetic first-order phase transitions, to be discussed further on, where magnetic domains play an equivalent role, Δx is the characteristic magnetic domain dimension. The same may also prove to the case of domain structures in superconductivity.

to a constant driving force) then during the next time interval $t_2 \rightarrow t_3$ where $t_3 - t_2 \sim \tau'$, if the freezing rate slows down, the corresponding effect will be that the number of heat sources lessens and becomes smaller than n_1. Therefore, as the freezing process continues, latent heat is evolved continuously with a *slight* variation between certain maximum and minimum values.

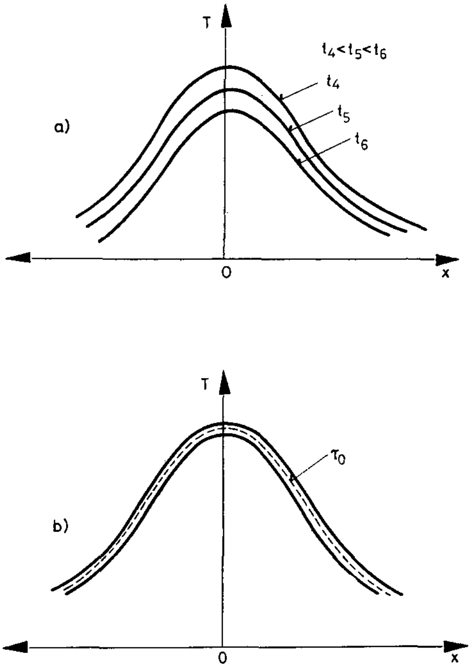

Fig. 6. (a) Temperature distribution as $f(x, t)$ following a single heating pulse. (b) Temperature distribution due to continuous heating pulses

However, the freezing of the sample in a portion of width d causes a brief temperature rise, which we shall call the pulse temperature $T_0 d$ [13–15]. It is quite obvious that Eq. (2) can be applied for the calculation of the distribution of the temperature $T(x, t)$ with the following approximation.

Equation (2) is the distribution function of temperature as a function of position x and time t. With a single heating pulse, the function would change with time as in Fig. 6(a), shown for instants of time t_4, t_5, t_6 where $t_4 < t_5 < t_6$. But the freezing process is continuous, with continuous heating pulses as assumed above. Consider therefore one period of the freezing process ($t_1 \rightarrow t_2 \rightarrow t_3$). The temperature distribution function changes from the upper curve of Fig. 6(b) (maximum heating effect) to the lower curve (minimum heating effect) and the same happens during the other period of the freezing process. Hence at any instant of time, the function lies between these two curves, and an average value (τ_0) can be assigned for t. Thus at any instant, the temperature distribution can be approximated by $T(x, \tau_0)$ (the dotted line in Fig. 6(b)) and so can be reckoned as a function of position x only.

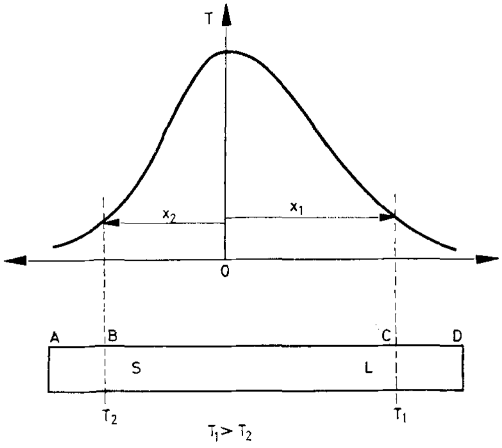

Fig. 7. Temperature distribution along the rod AD when the interface is at 0, where 0 is a distance x_1 from the thermocouple at C and x_2 from the thermocouple at B

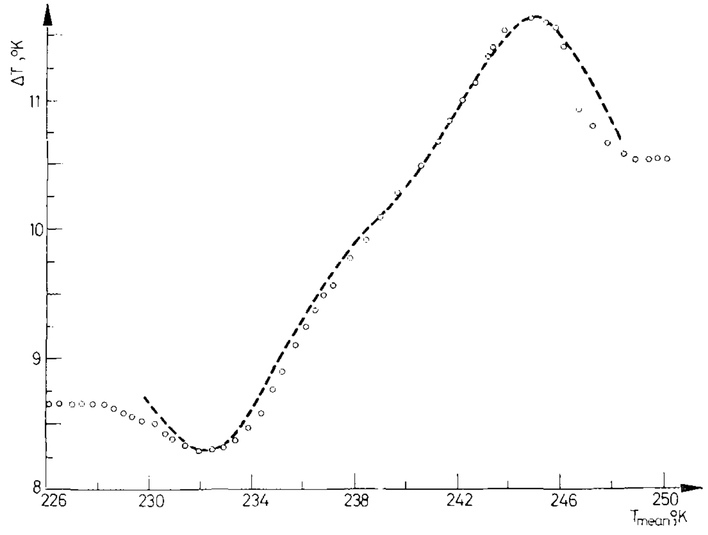

Fig. 8. $\Delta T - T$ curve obtained by melting mercury in the presence of a temperature gradient much larger than was used for obtaining the curve of Fig. 2. The dotted line is the theoretical curve

Figure 7 shows at a certain instant the interface advanced to the position 0 which is at a distance x_1 from thermocouple at C and x_2 from thermocouple at B. Because of the latent heat evolved during freezing, the true temperature gradient (instead of being $(T_1 - T_2)$ due to the external heater) should be the difference between $T_1 + (T_0)_L d(4\pi\alpha_L\tau_0)^{-1/2} \exp(-x_1^2/4\alpha_L\tau_0)$ and $T_2 + (T_0)_S d(4\pi\alpha_S\tau_0)^{-1/2} \exp(-x_2^2/4\alpha_S\tau_0)$. Physically, the pair of opposed extrema correspond to the passage of the interfacial boundary region past each thermometer in turn. Mathematically this corresponds to the exponential term of the theoretical expression reaching an extremal value of unity as the variable $x \to 0$.

The dotted lines of Fig. 2 are theoretical curves obtained on applying the above assumptions to the case of a mercury rod. The diameter of the uniform rod was 0.6 cm, with AB = 0.8 cm, BC = 3.6 cm, CD = 1.2 cm, and AD = 5.6 cm. In addition, the following physical parameters for solid and liquid mercury (taken from standard tables) were used in carrying out the calculation [29]:

Q (latent heat) = 11.3 $\mathrm{Jg^{-1}}$
ρ (density) = 13.5 $\mathrm{gcm^{-3}}$
$K_{(S)}$ (thermal conductivity) = 94×10^{-3} watts $\mathrm{cm^{-1}K^{-1}}$
$C_{(S)}$ (specific heat) = 0.134 $\mathrm{Jg^{-1}K^{-1}}$
$K_{(L)} = 70.6 \times 10^{-3}$ watts $\mathrm{cm^{-1}K^{-1}}$
$C_{(L)} = 0.121$ $\mathrm{Jg^{-1}K^{-1}}$

where $\alpha = K/C\rho$ and $T_0 = Q/C$. The only unknown parameters in the expression are d and τ_0. The best fit with the experimental data (Fig. 2) was obtained for $d \sim 1.7 \times 10^{-2}$ cm and $\tau_0 \sim 10$ sec. These values are quite close to the directly observed ones for bismuth and lead (10^{-2} cm, and a few seconds), although the experimental arrangement used for the latter measurements is different from ours. The step change at 234.84°K on the lower curve of Fig. 2 is due to supercooling.

Several other experiments were performed on mercury under different conditions. Figure 8 shows the result of a melting experiment with initial ΔT of 8.66°K in the solid state and 10.54 deg. in the fully-molten state. In this case the dimensions are AB = 1.1 cm, BC = 4.5 cm, CD = 0.9 cm and the uniform diameter = 0.3 cm. The agreement between the temperature-dependences of the experimental curve and the one obtained using Eq. (2) is reasonable, and values of 4.3×10^{-2} cm for d and of 10 sec for τ_0 resulted. It is interesting to note that the prominent undulation which develops along that part of the experimental curve lying between the extremal peaks is also displayed by the theoretical curve. This feature of the curve is mainly a result of the big temperature gradient employed.

We have also applied our model to the case of *magnetic* first-order phase transitions. Full experimental details are given elsewhere of the application of our new DTA technique to the case of antiferromagnetic chromium at its first-order spin-flip transition at 122°K (−151°C) [6]. This transition is very weak, the latent heat absorbed on warming being only 4 or 5×10^{-4} $\mathrm{Jg^{-1}}$ [30, 31]. In addition to the usual twin-peak effect illustrated by Fig. 9, extra structure appeared in the curve caused by regions of sample inhomogeneity. The form of Fig. 9 suggests

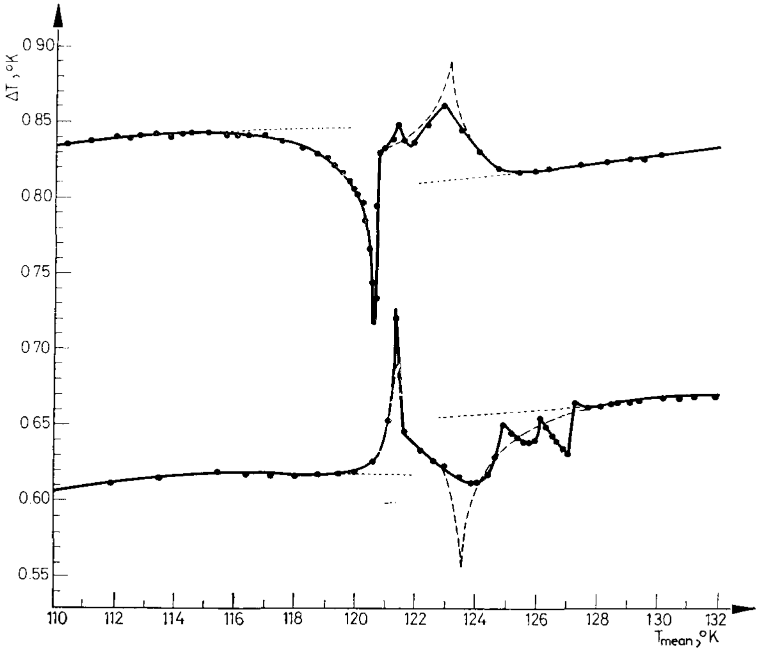

Fig. 9. Application of the new DTA technique to the weak magnetic first-order phase transition near 122°K in chromium. The latent heat is only 4 or 5×10^{-4} Jg^{-1}. The additional structure in these thermal curves is caused by inhomogeneities located towards one particular end of the sample (near the second thermocouple junction)

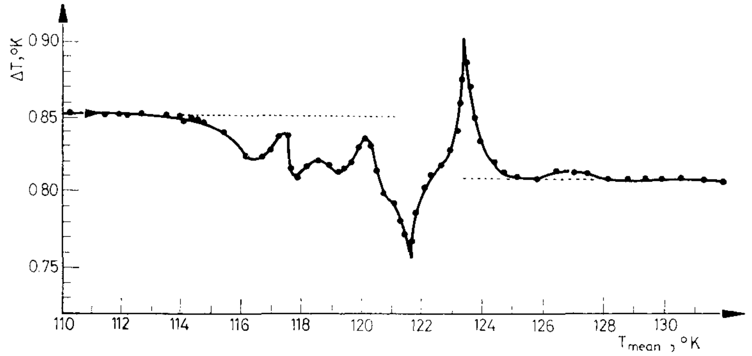

Fig.10. Endothermic curve for chromium; the upper curve of Fig. 9, but with the difference that the sample has been bodily reversed in position while leaving the heater and thermocouple geometry unchanged. Hence the less homogeneous part of the sample now affects mainly the first thermocouple instead of the second

that this less-homogeneous part of the sample is located in the neighbourhood of the second junction of the differential thermocouple pair (i.e. towards the end more remote from the heater end). This was later confirmed by Laue X-ray diffraction work which showed this part of the specimen to be more strained and to have smaller crystallites than the rest of the specimen. The result of an additional experiment, carried out on the chromium with it turned around with respect to the thermocouples and the specimen heater, is given in Fig. 10. It is evident that this reversal has the effect of siting the inhomogeneous part of the chromium near the thermocouple at the higher instead of at the lower temperature. The dashed curves in Fig. 9 are drawn to indicate the behaviour thus expected of a strain-free specimen.

In the magnetic spin-flip transition the main difference compared with the solid $\rightleftharpoons$ liquid transition is that the latent heat depends chiefly on the change in the magnetic entropy. In a simple sense, on passing through the spin-flip transition, the magnetic domains change from one configuration to another, resulting in a change of internal energy [30, 31]. Recently, the characteristic domain dimension of chromium [32] has been observed visually by the X-ray double-crystal method at liquid nitrogen temperature to be ~ 1 mm [33]. For the reasons given above, we therefore take $d \sim 1$ mm and, from Fig. 9,

$$\Delta T(x = 0, \tau_0) \sim T_0 d(4\pi\alpha\tau_0)^{-1/2} \sim 0.1^\circ\mathrm{K}$$

The following known values were used for the other relevant parameters:

Q (latent heat) $\sim$ 4 or 5×10^{-4} J/g [30, 34]
$K_{(T<T_F)} \sim K_{(T>T_F)} \sim 1.28$ watts $\mathrm{cm}^{-1}\mathrm{K}^{-1}$ [35]
$C_{p(T<T_F)} \sim C_{p(T>T_F)} \sim 0.116$ $\mathrm{Jg}^{-1}\mathrm{K}^{-1}$ [36]
ρ (density) = 7.21 gcm^{-3}

We found that $\tau_0 \sim 10^{-9}$ sec resulted. Physically, it is reasonable to relate this time constant to the relaxation time for magnetic domains to return toward equilibrium after the disturbance of the domain configuration on passing through T_F. For such a relaxation process, the relaxation time can also be calculated from ultrasonic attenuation measurements. Later, such measurements were made on chromium, and the result obtained (a relaxation time no shorter than $\sim 10^{-10}$ sec) [37] directly confirmed our value within an order of magnitude. As a consequence, it appears that magnetic domains in the phase boundary region play a role equivalent to that of the microstructure of the interface region at the point of fusion.

Additional experimental remarks

In the previous sections we have demonstrated some of the uses to which the new DTA method may be put. It may be used for detecting phase transitions, even very weak ones, and for indicating their temperature of occurrence. Moreover, information is simultaneously provided about the internal microscopic processes taking place at the transition, including diffusional relaxation times and the volume of the heat sources or sinks. We have also indicated, using a particular chromium sample for illustration, how an inhomogeneous part of an otherwise supposedly pure sample can manifest its presence by the effect that it produces on the curve. The next figure (Fig. 11) illustrates the consequence of deliberately adding an "impurity" to the central part of an indium rod which is then caused to melt in the presence of a temperature gradient. The "impurity" was a horizontal platinum wire of diameter 0.5 mm passing through the polyethylene container wall and thus into the indium specimen about midway between the thermocouple probes. The effect was to produce some fine structure on the curve corresponding to the time interval during which the advancing liquid-solid interface arrives at and passes the transverse platinum wire. It appears that the disturbance deliberately introduced into the middle of the sample does not affect the curve as a whole, but modifies that small part of it corresponding to the time taken for the interfacial region to pass through the disturbed region.

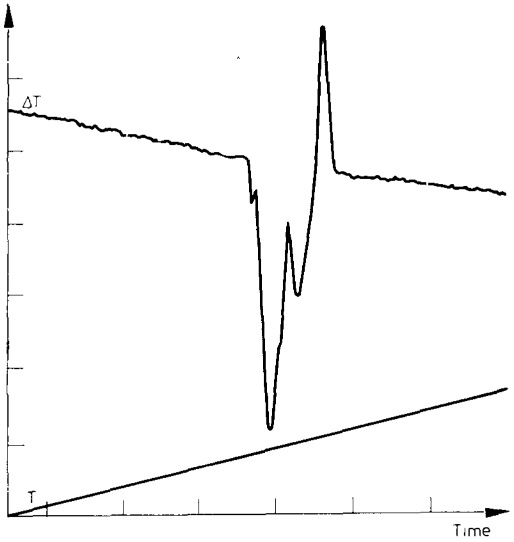

Fig. 11. $\Delta T - T$ curve for melting indium showing the effect of deliberately locating a "disturbance" in the specimen midway between the thermocouple probes

In the previous section, we indicated that it is advisable to locate the heater at the upper end of the vertical sample if transitions other than solid $\rightleftarrows$ solid ones are to be studied. This is because, in a solid → liquid transition for a substance whose solid density exceeds the liquid density, if the lower end of the sample is melted first gravitational effects will cause circulation currents in the liquid state to develop. The variability of such currents prevents a uniform passage of heat through

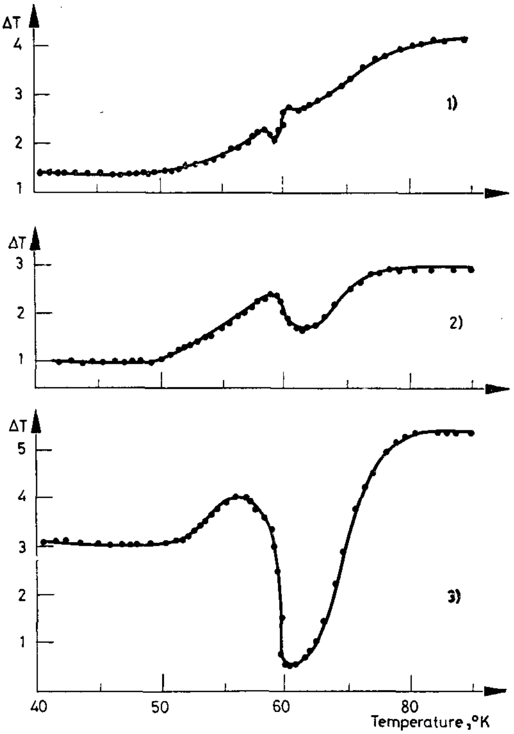

Fig. 12. Heating $\Delta T - T$ curves for orthorhombic uranium following rapid quenching from 80° to 4°K. Rates of quenching were (1) 0.23°K sec.$^{-1}$,(2) 0.47°K sec.$^{-1}$, and (3) 0.73°K sec.$^{-1}$. A low-temperature metastable structure reverts exothermically to a more stable form in the neighbourhood of 55° to 60°K

the sample, and the microscopic behaviour at the melting interface is rendered uncertain. The only stable means of studying melting phenomena in substances which are less dense when liquid than when solid is by having the temperature gradient in the same sense as the gravitational field (the opposite would seem to be the case for the ice → water transition).

Figure 12 is another example of the application of our DTA technique to the study of the solid state, showing heating $\Delta T - T$ curves obtained on α-uranium after quenching to liquid helium temperatures (4°K). More rapid quenching rates raise the fraction of a metastable low-temperature phase that is formed. Subsequent reheating permits a reversion of this phase at around 55 to 60°K to the form normally stable at these higher temperatures. The quenching rates from 80 to 4°K, which were employed prior to obtaining curves 1, 2 and 3, were respectively 0.23°K sec^{-1}, 0.47°K sec^{-1}, and 0.73°K sec^{-1}. The twin-peaks develop quickly as the available latent heat from the crystal phase conversion increases. From the nature of the peaks it is clear that this heat is exothermic.

Conclusion

This paper has reported a new DTA technique which does not require a reference sample. By virtue of a temperature gradient imposed across the test sample, the test sample is made to serve as its own reference. The method might therefore be termed auto-differential analysis. It provides a characteristic effect at the time of occurrence of endothermic or exothermic reactions which enables useful information about the nature of the concurrent internal processes to be deduced. The method is simple and does not necessarily demand special, complex and expensive equipment, and yet for physical phenomena such as melting or crystalline phase transitions the reproducibility is excellent. Furthermore, by an elementary extension of the technique, derivative curves of our DTA curves having their own intrinsic characteristics and uses may be generated. It is therefore expected that our new technique will be of interest to research and industrial analysts in many scientific, medical and industrial disciplines.

*

We wish to acknowledge support of this research by the National Research Council of Canada and Dalhousie University, Halifax.

References

1. W. C. Roberts-Austen, Proc. Instn. mech. Engrs., (1899) 35.
2. W. C. Roberts-Austen, Nature, 59 (1899) 566.
3. H. Le Chatelier, Compt. rend. Acad. Sci. (Paris), 104 (1887) 1443.
4. H. Le Chatelier, Revue Métall. (Paris), 1 (1904) 134.
5. Refer, for example, to R. C. MacKenzie in Differential thermal analysis (edited by R. C. MacKenzie, Academic Press, London and New York, 1970) Chapter 1.
6. G. T. Meaden and N. H. Sze, Phys. Rev. Letters, 23 (1969) 1242.
7. N. H. Sze and G. T. Meaden, Phys. Letters, 37A (1971) 393.
8. G. T. Meaden and N. H. Sze, Canad. Research and Development, 5 (1972) No. 3, p. 13.
9. N. H. Sze, Ph. D. Thesis, Dalhousie University, Halifax (1972), to be published.
10. H. S. Carslaw and J. C. Jaeger, Conduction of heat in solids, Clarendon Press, Oxford, 1959.
11. For example, (a) heat balance integral method, T. R. Goodman, Trans. Amer. Soc. Mech. Engr., 80 (1958) 335; T. R. Goodman and J. J. Shea, J. Appl. Mech., 27 (1960) 16; G. Poots, Int. J. Heat Mass Transfer, 5 (1962) 525.
   (b) variational method, M. A. Biot and H. Daughaday, J. Aerospace Sci., 29 (1962) 227.
   (c) method of moving heat sources, F. Jackson, J. Heat transfer, 87C (1965) 329.
12. For example, V. Paschkis, Trans. Amer. Foundryman's Soc., 53 (1945) 90, 61 (1953) 142; Proc. Inst. British Foundry, A44 (1951) 32; R. M. Howe and V. S. Haneman, Proc. Inst. Radio Eng., 41 (1953) 1497; A. L. London and R. A. Seban, Trans. Amer. Soc. Mech. Eng., 64 (1943) 771; F. Kreith and F. E. Romie, Proc. Phys. Soc., 68 (1955) 277; W. D. Murray and F. Landis, Trans. Amer. Soc. Mech. Eng., 81 (1959) 106.
13. E. L. Woisard, J. Appl. Phys., 32 (1961) 40.
14. J. Oualid, J. de Physique, 2 (1960) 124.
15. E. L. Foley and R. B. Sawyer, J. Appl. Phys., 35 (1964) 3053.
16. J. Fourier, The Analytical Theory of Heat, Dover, New York, 1955.

17. A. V. Luikov, Analytical heat diffusion theory, Academic Press, New York and London, 1968.
18. D. A. Petrov, Zh. Fiz. Khim., 30 (1956) 50.
19. B. Chalmers, Principles of Solidification, Wiley, New York, 1964.
20. A. I. Landau, Fiz. Met. Metall., 6 (1958) 148.
21. B. M. Turovskii and Milvidskii, Fiz. Tverd. Tela, 3 (1961) 2519 (Sov. Phys. Solid State, 3 (1961) 1834).
22. J. J. Gilman, The Art and Science of Growing Crystals, Wiley, New York, 1963.
23. G. V. Komarov and A. R. Regel, Fiz. Tverd. Tela, 5 (1963) 773 (Sov. Phys. Solid State, 5 (1963) 563).
24. J. A. Burton, S. D. Kolh, W. P. Slichter and J. D. Struthers, J. Chem. Phys., 21 (1953) 1991.
25. L. S. Milevskii, Kristallografiya, 6 (1961) 249 (Sov. Phys. Crystallography, 6 (1961) 193).
26. J. M. Bardeen and B. S. Chandrasekhar, J. Appl. Phys., 28 (1958) 1372.
27. W. G. Pfann, K. E. Benson and J. H. Wernick, J. Electronics, 2 (1957) 597.
28. S. A. Semenkovich, L. A. Kolomets and N. V. Kolomets, Sov. Phys. Solid State, 3 (1961) 1159.
29. J. A. Bailey and J. R. Davila, J. Inst. Metals, 97 (1969) 248.
30. R. Street, B. C. Munday, B. Window and I. R. Williams, J. Appl. Phys., 39 (1968) 1050; A. R. Pepper and R. Street, Proc. Phys. Soc., 87 (1966) 971.
31. R. Street, Phys. Rev. Letters, 10 (1963) 210; R. A. Montalvo and J. A. Marcus, Phys. Letters, 8 (1964) 151; S. A. Werner, A. Arrott and H. Kendrick, Phys. Rev., 155 (1967) 528.
32. C. Akiba and T. Mitsui, J. Phys. Soc. Japan, 32 (1972), show that the domain size increases with sample purity
33. S. Hosoya and M. Ando, Phys. Rev. Letters, 26 (1971) 321.
34. M. O. Steinitz, L. H. Schwartz, J. A. Marcus, E. Fawcett and W. A. Reed, Phys. Rev. Letters, 23 (1969) 979.
35. G. T. Meaden, K. V. Rao, H. Y. Loo and N. H. Sze, J. Phys. Soc. Japan, 27 (1969) 1073.
36. R. H. Beaumont, H. Chihara and J. A. Morrison, Phil. Mag., 5 (1960) 188.
37. M. Roth, M. Sc. Thesis, Dalhousie University, Halifax (1971).

Résumé — On décrit et discute une nouvelle technique d'ATD en considérant sa fonction, son utilisation, ses possibilités, sa théorie et son application. On indique les processus internes qui se produisent lors de l'absorption ou de la libération d'énergie. Les principales caractéristiques de la technique se rapportent à la sensibilité élevée et à l'indépendance de l'échantillon de référence.

Zusammenfassung — Eine neue differentialthermoanalytische Technik wird hinsichtlich ihrer Funktion, Arbeitsweise, Leistung, Theorie und Anwendung beschrieben. Es wird über die Beschaffenheit der inneren Vorgänge bei der Energie-Absorption oder -Freisetzung berichtet. Vorteile der neuen Technik sind die hohe Empfindlichkeit und die Unabhängigkeit von der Referenzprobe.

Резюме — Описана и обсуждена в отношении функции, операции, выполнения, теории и использования новая дифференциальная термоаналитическая методика, обеспечивается информация о природе процессов, происходящих при поглощении или освобождении энергии. Важными особенностями методики являются высокая чувствительность и независимость эталонного образца.